Supporting information

Photochemical transformation of poly(butylene adipate-co-terephthalate) and its effects on enzymatic hydrolyzability

Guilhem X. De Hoe[1†], Michael T. Zumstein[2†x], Gordon J. Getzinger[2], Isabelle Rüegsegger[2], Hans-Peter E. Kohler[3], Melissa A. Maurer-Jones[2§], Michael Sander[2] *, Marc A. Hillmyer[1] *, and Kristopher McNeill [2] *

[1]Department of Chemistry, University of Minnesota,
Minneapolis, Minnesota 55455-0431, United States

[2]Institute of Biogeochemistry and Pollutant Dynamics, ETH Zurich,
8092 Zurich, Switzerland

[3] Environmental Microbiology, Swiss Federal Institute of Aquatic Science and Technology (Eawag), 8600 Dübendorf, Switzerland

[†] These authors contributed equally and are listed alphabetically.
[x] Current address: School of Civil and Environmental Engineering, Cornell University, Ithaca, NY, 14853, USA
[§] Current address: University of Minnesota Duluth, Duluth, Minnesota 55812, USA
*To whom correspondence should be addressed:
E-mail: michael.sander@env.ethz.ch, phone: +41-(0)44 6328314
E-mail: hillmyer@umn.edu, phone: +1-612-625-7834
E-mail: kris.mcneill@env.ethz.ch, phone: +41-(0)44 6324755

In preparation for submission to *Environmental Science and Technology*

Number of pages: 31
Number of figures: 24

Section S1. Materials and Methods

Chemicals. Potassium chloride (KCl, product number: P4504), terephthalic acid (185361), pyridine (Pyr, 270407), deuterated chloroform ($CDCl_3$, 151823**),** and hydrochloric acid (HCl, 30721) were obtained from Sigma-Aldrich. Chloroform (C/4966/17) and acetonitrile (A/0627/17) were obtained from Fisher Chemical. 4-nitroanisole (PNA, 10354-3), 2-(2-benzotriazolyl)-4-methylphenol (533203), and 4-benzoylbenzoic acid (1240-7) were obtained from Aldrich. 1,4-dimethoxybenzene (D0629) was obtained from TCI.

Actinometry. To control the intensity of the Rayonet photoreactor, we performed PNA/Pyr-based actinometry.[1] For a typical actinometry procedure, a borosilicate glass test tube (VWR, PYREX, 99445-15) was charged with 10 µL of a PNA solution (10 mM in acetonitrile), 50 µL of a pyridine solution (100 mM in acetonitrile), and 9.94 mL of Milli-Q water. The test tube was then transferred into the carousel sample holder of the photo reactor. The remaining positions of the sample holder were filled with test tubes containing water only. The irradiation was performed with eight bulbs (maximal light intensity at 300 nm) while the carousel was rotating. At specific times during the irradiation, a 150 µL aliquot of the PNA/Pyr solution was transferred into an amber vial, which was subsequently stored in the dark at 4 °C.

To determine the concentration of PNA in the irradiated solutions, we used an Agilent 1100 Series HPLC equipped with a ZORBAX Eclipse XDB C18 column (4.6 x 150 mm, Agilent 993967-902), a C18 guard column (4.6 x 12.5 mm, Agilent 820950-926), and a G1314A UV detector (absorbance measured at 316 nm). The aqueous fraction of the mobile phase consisted of acetate buffer (30 mM acetate/acetic acid, pH 6.0) containing 5% (v/v) acetonitrile, while the organic fraction was pure acetonitrile. Throughout the time of the experiment (4.5 min), the organic fraction of the mobile phase was constantly held at 70%, the flow rate at 1 mL/min. Absorbance peaks were integrated with the Agilent OpenLAB CDS ChemStation Edition C.01.05 software. PNA concentrations were calculated based on calibration solutions ranging between 1 and 20 µM.

Liquid extraction and ^{1}H-NMR analysis of hydrolysis products. We complemented our HPLC-HRMS-based analysis of the hydrolysis products with ^{1}H nuclear magnetic resonance (NMR) spectroscopy. Therefore, we thawed the solutions that were stored after the pH-stat titration experiments and added a few drops of HCl

solution (1 M) to 0.75 mL of the solution containing the hydrolysis products (resulting pH < 1.5). For the extraction of the hydrolysis products, we added 0.75 mL of deuterated chloroform ($CDCl_3$) to the acidified samples and vortexed the resulting mix for 15 s. The organic phase was then transferred into a sample tube for the NMR measurement. Chloroform addition, vortexing, and transferring of the organic phase were repeated twice. For absolute quantification of the hydrolysis products, we added a solution of 1,4-dimethoxybenzene as an internal standard to our analytes. ^{1}H-NMR spectra were acquired on a Bruker, Avance III 400 MHz NMR spectrometer equipped with a 5 mm BBFO Z-Gradient high-resolution probe (relaxation time was set to 15 s). All ^{1}H-NMR spectra were baseline and phase corrected. The chemical shifts were referenced to the proton of $CHCl_3$ that is present in $CDCl_3$.

Quantification of hydrolysis by TOC measurements. Complementary to the pH-stat titration experiments, we used an approach based on quantifying the total organic carbon (TOC) of a solution to study the hydrolysis of PBAT films. For these experiments, we punched a circular film piece (diameter 2.3 cm) out of the blown PBAT film and incubated this piece at 40 °C in a 20 mL glass vial containing 15 mL of buffer (90 mM potassium phosphate, 10 mM potassium chloride, pH 7.0, filtered at 0.22 µm). Incubations were performed in the dark under orbital shaking at 140 rpm. 50 h after the addition of the PBAT films, we added a stock solution of *Fusarium solani* cutinase (300 µL; final concentration: 82 µg FsC/mL). At indicated times during the experiment, we took 250 µL of the incubation solution into a 1.5 mL plastic tube and stored these aliquots at 4 °C. After all samples had been collected, we centrifuged the samples (2000 x g, 3 min) to make sure that PBAT particles that potentially detached from the film were collected at the bottom of the tube. Subsequently, we transferred 80 µL from the top of the solution into a test tube for TOC measurements, added Milli-Q water to a total volume of 8 mL, and measured these solutions with a TOC analyzer (TOC-L, Shimadzu). The obtained signal was converted to a TOC concentration employing a standard calibration curve (0 to 20 mg C/L) prepared from a TOC standard (Sigma-Aldrich, 76067).

Irradiation of PBAT films by sunlight. Blown films of PBAT were cut into pieces of 8 x 8 cm. We then stapled these films onto a EUR-palette that was placed at a shade-free location on the roof of our institute's building in Zurich, Switzerland. At indicated times, we sampled films and stored them in the dark until we determined their

gel fraction. We determined the gel fraction of PBAT films that were irradiated by sunlight, and of films that were irradiated in the photoreactor on one side. These measurements were performed differently than the gel fraction measurements described in the manuscript. For the former measurements, we stuffed disposable glass Pasteur pipets with glass wool and determined its mass (m_1). We then added the PBAT film (approximately 12 mg) onto the glass wool and determined its mass (m_2). Subsequently, we loaded the pipet with chloroform, incubated it at room temperature for 1 h, and pushed the chloroform out of the pipet. Then, the pipet was washed three times with chloroform, dried at 70 °C (1 h), and mass its mass (m_3) was determined. We calculated the gel fraction as $(m_3-m_1)/(m_2-m_1)$.

Differential scanning calorimetry (DSC). DSC was performed on the untreated and irradiated PBAT films using a TA Instruments Discovery Series differential scanning calorimeter. Samples subjected to calorimetry (ca. 4 mg) were placed in T-Zero hermetic pans and cooled to –80 °C before the first and second heating ramp to 250 °C; all temperature sweeps were performed at 10 °C min^{-1}. We used the *Trios* software to determine the glass transition temperatures (midpoints of each transition) and the melting temperatures (maximum of the endotherm). These temperatures were measured using the first heat so as to account for the thermal history from the PBAT film processing conditions.

Wide-angle X-ray scattering (WAXS). Room-temperature WAXS data were collected on the Dupont-Northwestern-Dow Collaborative Access Team (DND-CAT) insertion device beamline at Sector 5 of the Advanced Photon Source at Argonne National Laboratory, using 17 keV X-rays (λ = 0.7293 Å) and a sample-to-detector distance of 201.31 mm. PBAT films (original thickness 0.025 mm), both untreated and irradiated, were folded to generate squares of PBAT with thicknesses of 0.1 mm, which were sandwiched between two layers of Kapton tape and mounted to Teflon washers. Each sample was exposed to the beam for 5 s; isotropic scattering patterns were azimuthally averaged to give one-dimensional plots of scattered intensity I as a function of the scattering wavevector q. Scattered intensity was calibrated using a glassy carbon standard and q was calibrated using a silicon diffraction grating. The raw scattering data for 2 sheets of Kapton tape was subtracted from the raw sample data, which was then corrected for the actual sample thickness (i.e., 0.1 mm).

Size-exclusion chromatography (SEC). SEC was performed at 35 °C using an HP/Agilent 1100 series size-exclusion chromatograph equipped with a HP 1047A refractive index detector. The mobile phase was chloroform (1 mL min^{-1} flow rate); prior to reaching the detector, the sample passed through a PLgel 5 μm guard column before passing through three successive PLgel Mixed C columns. We used a 10-point calibration curve generated using EasiCal polystyrene standards purchased from Agilent to determine M_n and $Đ$ for untreated PBAT and the sol fractions of UV-irradiated PBAT.

Solvent casting of PBAT films. We dissolved PBAT in chloroform to obtain a 0.5 % (w/w) solution. For photostabilized films, we added 2-(2-benzotriazolyl)-4-methylphenol (BMP) to the solution to a final concentration of 0.0001 % (w/w, BMP/chloroform) and horizontally orbit-shook the solution (40 min). To obtain solvent-cast PBAT films, we added 27 mL of the solution to a glass petri dish (diameter 9.1 cm) and evaporated the chloroform by horizontally orbit-shaking the petri dish at 100 rpm in the fume hood for 14 h. To release the film from the petri dish, we dipped the dish into liquid nitrogen and then carefully peeled the film from the dish and stored in the dark until the hydrolysis experiments.

Section S2. Results and Discussion

Characterization data for untreated PBAT

To investigate the molar mass distribution and thermal properties of the untreated PBAT film, we respectively employed size exclusion chromatography and differential scanning calorimetry (**Figures S1** and **S2**). The size exclusion chromatography was performed using a chloroform mobile phase, and the molar mass distribution was evaluated with respect to polystyrene standards; the number average molar mass was determined to be 37 kg/mol with a dispersity of 2.2. The differential scanning calorimetry profile for the first heating cycle revealed a glass transition temperature at –30 °C as well as a broad melting transition containing two maxima at 59 °C and 121 °C. These maxima respectively represent the melting of adipate-rich crystallites and terephthalate-rich crystallites. [2] We note that the latter of these crystallite types is the one that is predominantly observed by wide angle x-ray scattering (discussed later in the Supplementary Information). Overall, the thermal properties and scattering signals are consistent with prior literature reports. [2-4]

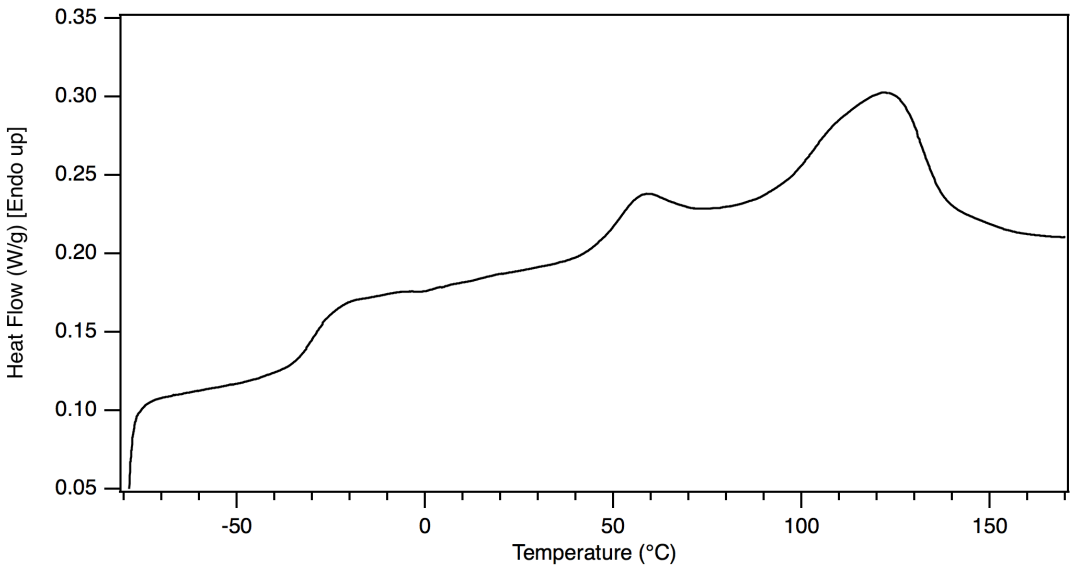

Figure S1. Differential scanning calorimetry trace of untreated poly(butylene adipate-co-terephthalate), which shows a glass transition at –30 °C and a broad melting transition between 40 °C and 150 °C.

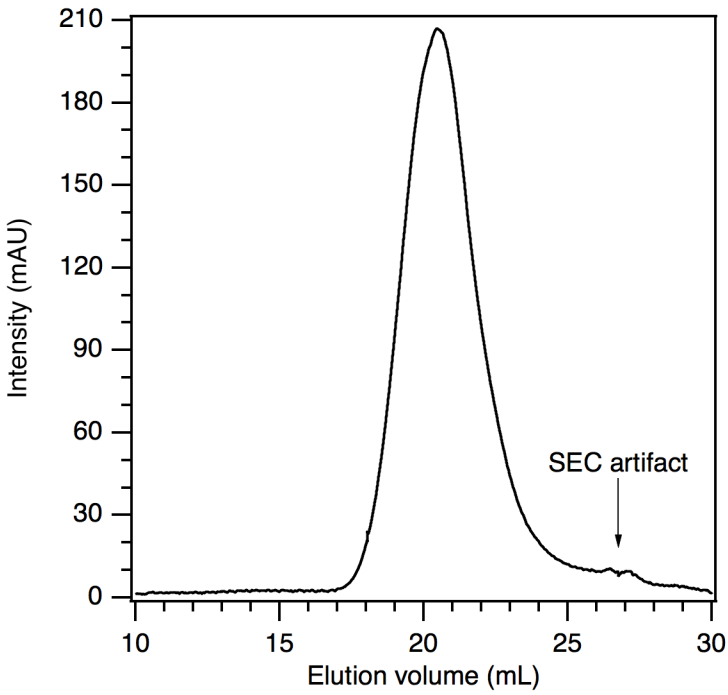

Figure S2. Size exclusion chromatography trace (chloroform mobile phase) of untreated poly(butylene adipate-co-terephthalate).

To determine the chemical composition of the poly(butylene adipate-co-terephthalate) (PBAT) film used in this manuscript, we dissolved a small piece in deuterated chloroform ($CDCl_3$) and analyzed the solution by ^1H nuclear magnetic resonance (NMR) spectroscopy (**Figure S3**). We used the integrals of the peaks corresponding to the –OC**H**$_2$– protons of butanediol (4.4 and 4.1 ppm, see spectrum for peak assignment) to determine the ratio of terephthalate units to adipate units (0.936).

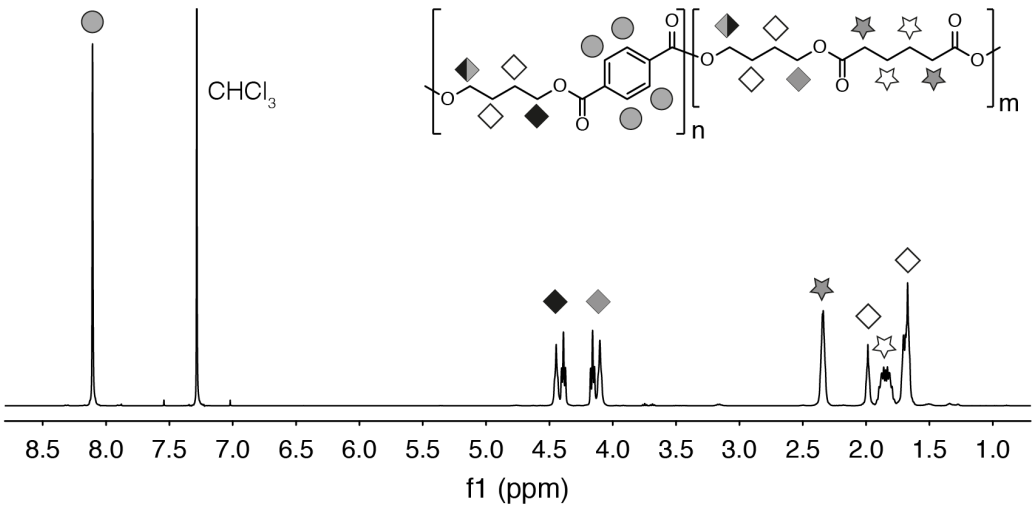

Figure S3. ^1H NMR spectrum ($CDCl_3$, 400 MHz) of a poly(butylene adipate-co-terephthalate) (PBAT) film. The symbols next to the peaks in the spectrum and next to the protons in the structural formula depict the peak assignment.

Spectrum of UV lamps

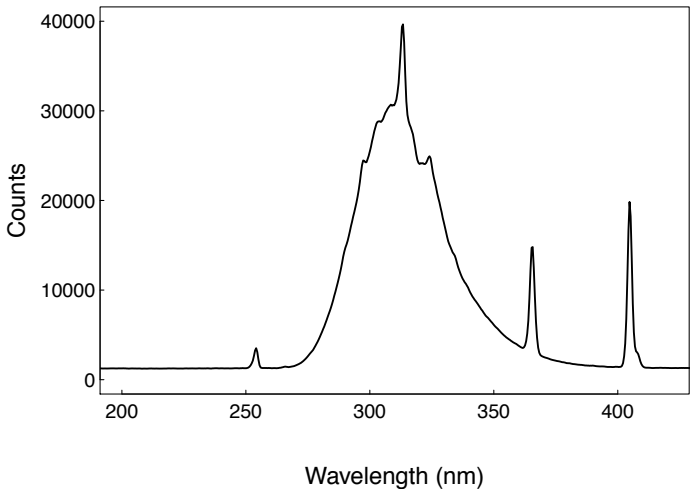

Figure S4. Spectrum emitted by the UV bulbs used in this study as measured with a Jaz Spectrometer (Ocean Optics).

Actinometry experiment

To confirm that the Rayonet photoreactor was providing light at a constant intensity, we performed actinonometry experiments before and after the irradiation of the PBAT films (**Figure S5**). We used the photochemical degradation of 4-nitroanisole (PNA) in a pyridine-containing solution to measure light intensity. The first-order rate constants were very similar between experiment 1 (0.0102 min^{-1}, before film irradiation) and experiment 2 (0.0103 min^{-1}, after film irradiation).

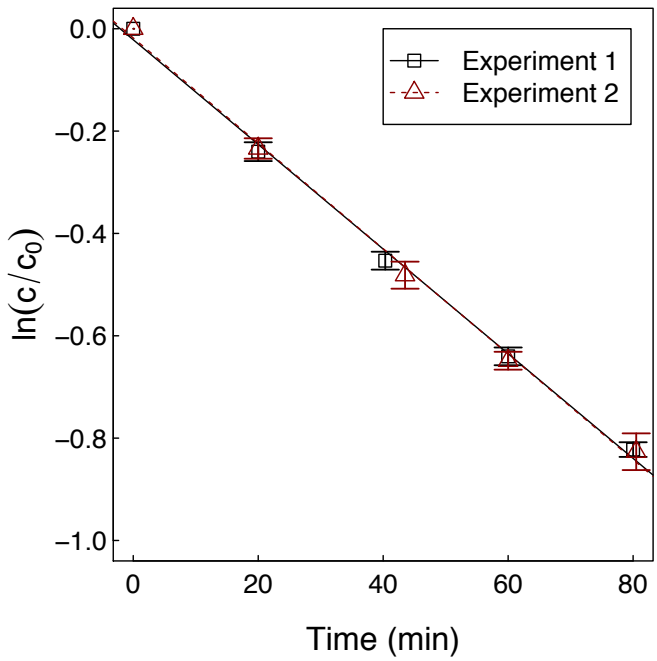

Figure S5. Logarithmic plot of the photochemical degradation of 4-nitroanisole (PNA) in a solution containing pyridine. Experiments 1 (black squares) and 2 (red triangles) were performed before and after the irradiations of the polyester films, respectively. Error bars represent standard deviations of triplicate measurements.

Quantification of photochemically produced acids by pH-stat titration

Upon the addition of poly(butylene adipate-co-terephthalate) (PBAT) films to the solution, we detected produced acids by automated pH-stat titration (**Figure S6**). While the addition of an untreated PBAT film did not result in the release of acid, the number of released acid increased with increasing irradiation time. The results of independent duplicate experiments demonstrated the reproducibility of the photochemical production of carboxylic acids.

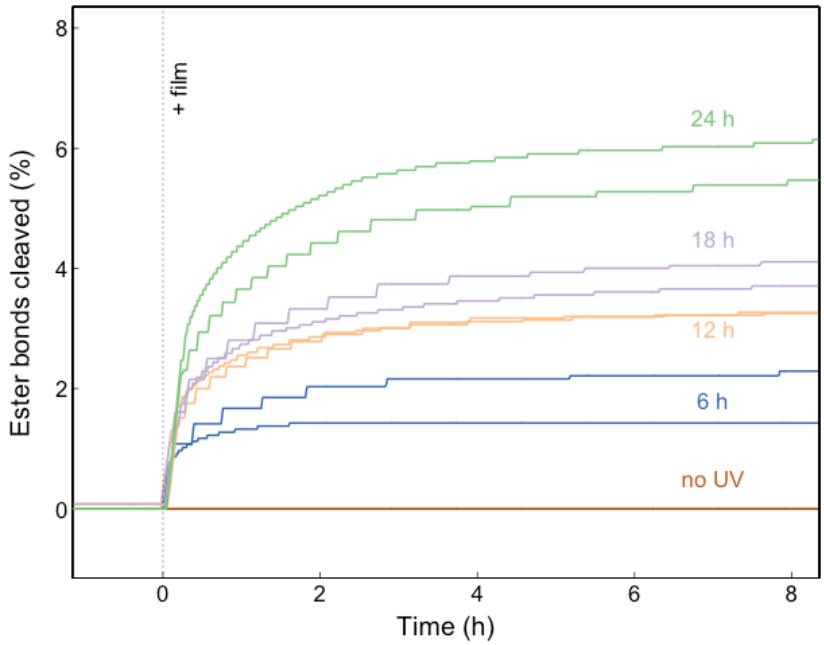

Figure S6. Cumulative number of released protons, relative to the number of ester bonds in the poly(butylene adipate-co-terephthalate) (PBAT) films, quantified by automated pH-stat titration. Each side of the PBAT film was irradiated with UV light for the time indicated next to the curve. PBAT films were added to the system at the time indicated by the vertical dashed line. Duplicate experiments are shown in the same color.

Quantification of enzymatically hydrolyzed ester bonds by pH-stat titration

After all the photochemically produced protons had been released into the solution (i.e., 24 h after addition of the PBAT film), we added *Fusarium solani* cutinase (FsC). This addition resulted in the hydrolysis of ester bonds of PBAT and the subsequent release of protons into the solution (**Figure S7**). The results of independent duplicate experiments demonstrated the reproducibility of the enzymatic hydrolysis of irradiated PBAT films.

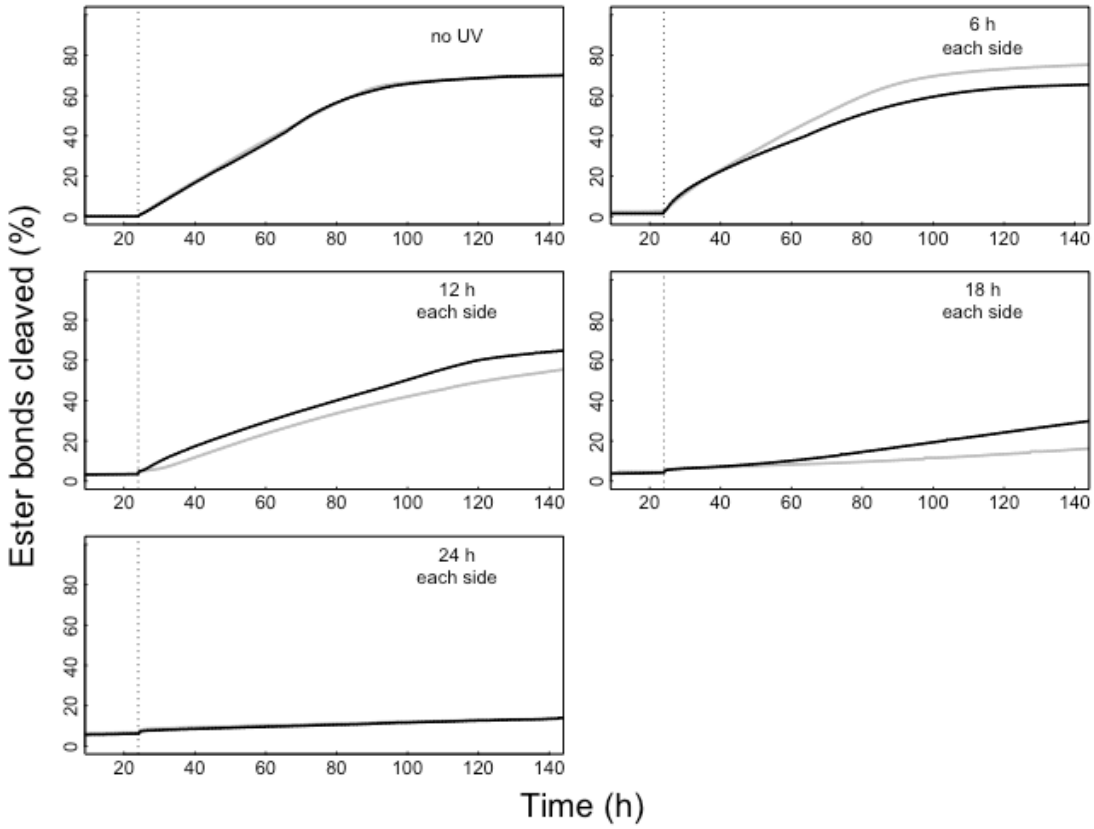

Figure S7. Hydrolysis of irradiated poly(butylene adipate-co-terephthalate) (PBAT) films by *Fusarium solani* cutinase (FsC). The plots show the cumulative number of released protons, relative to the number of ester bonds in the PBAT film, quantified by automated pH-stat titration. PBAT films were irradiated with UV light for the time indicated in each panel. FsC was added to the system at the time indicated by the vertical dashed lines. Duplicate experiments are depicted in black and grey.

Incomplete hydrolysis was not due to enzyme inactivation

To confirm that the incomplete hydrolysis of ester bonds in poly(butylene adipate-co-terephthalate) (PBAT) film by *Fusarium solani* cutinase (FsC) (i.e., only ~70% of the ester bonds in untreated films were hydrolyzed when the plateau was reached) was not due to enzyme inactivation, we added fresh cutinase solution when the hydrolysis plateau was reached (indicated by the dashed vertical line at 145 h in **Figure S8**). We note that the solution was clear at this stage indicating the complete transformation of the PBAT film into soluble hydrolysis products. The finding that the second addition of FsC did not increase the number of hydrolyzed ester bonds demonstrated that FsC did not hydrolyze a fraction of the ester bonds.

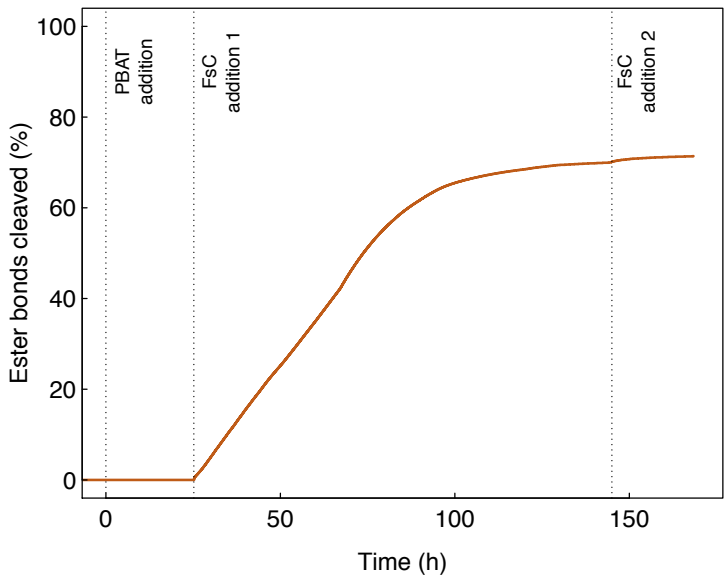

Figure S8. Hydrolysis of an untreated poly(butylene adipate-co-terephthalate) (PBAT) film by *Fusarium solani* cutinase (FsC). The plot shows the cumulative number of released protons, relative to the number of ester bonds in the PBAT film, quantified by automated pH-stat titration. PBAT film was added at t = 0 h. FsC was added to the system at the times indicated by the additional vertical dashed lines at t = 24 h and t = 145 h.

HPLC-HRMS-based product analysis of the enzymatic hydrolysis of PBAT

To identify the products of the enzymatic hydrolysis of untreated poly(butylene adipate-co-terephthalate) (PBAT) films by *Fusarium solani* cutinase (FsC), we analyzed the solution that remained after the pH-stat titration experiments by high-pressure liquid chromatography coupled to both high-resolution mass spectrometry and UV absorbance (HPLC-HRMS-UV). The strongest signals were assigned to adipate (A), terephthalate (T), and the butanediol-terephthalate dyad (BT) (**Figure S9**). Butanediol (B) was not detected. This analysis suggests that A, B, T, and BT are the predominant hydrolysis products of the hydrolysis of PBAT by FsC. The strong signal detected for BT, which contains an ester bond that was not hydrolyzed by FsC, supports the incomplete ester hydrolysis measured by automated pH-stat titration. To assess the presence of BT more quantitatively, we performed nuclear magnetic resonance (NMR) spectroscopy experiments (**Figure S10**).

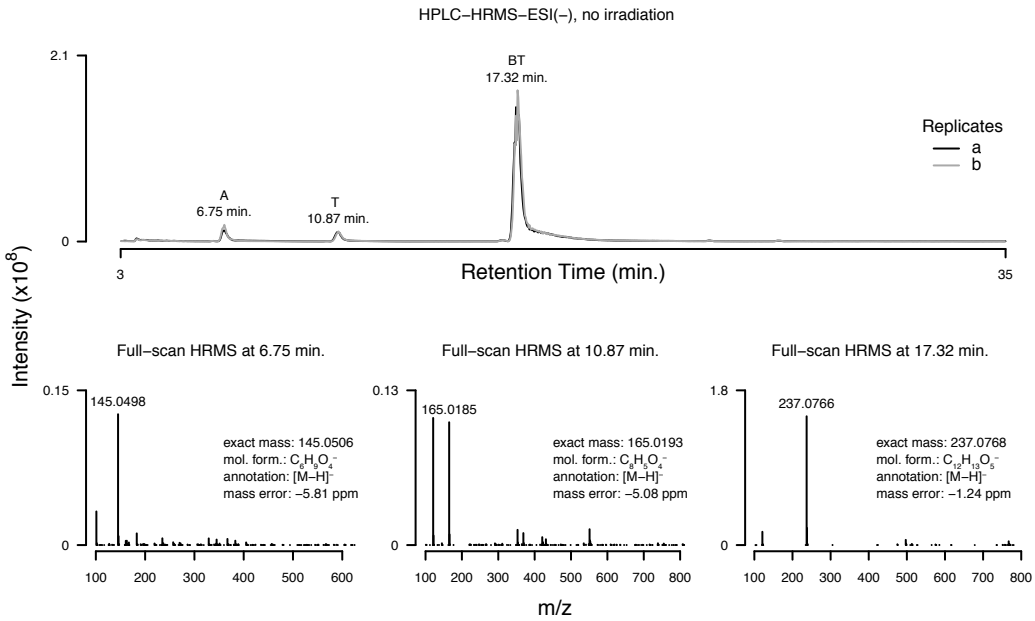

Figure S9. Product identification of the enzymatic hydrolysis of poly(butylene adipate-co-terephthalate) (PBAT). **Top**. Base peak chromatograms generated by high-pressure liquid chromatography coupled to high-resolution mass spectrometry (HPLC-HRMS) in negative mode electrospray ionization (ESI). Curves of independent duplicates (grey and black) overlap. **Bottom**. Full-scan HRMS spectra acquired at the indicated retention times; additional information on the molecule assigned to the predominant masses are provided in each panel.

^{1}H NMR analysis of the products from the enzymatic hydrolysis of PBAT

To confirm the high abundance of the butanediol-terephthalate dyad (BT) in the hydrolysis products of untreated PBAT, we liquid-liquid extracted the solution that remained after the pH-stat titration experiment and analyzed it by ^{1}H nuclear magnetic resonance (NMR) spectroscopy (**Figure S10**). The peaks indicative of the hydrolysis products were the aryl protons from terephthalate units and protons adjacent to a hydroxyl moiety; the integrals from these peaks (1:0.5:0.5) could be explained by the presence of pure BT or an equimolar mix of the terephthalate-butanediol-terephthalate triad (TBT) and butanediol (B). The finding that the peak ratio was the same for three consecutive extractions strongly suggests that BT was the predominant terephthalate-containing hydrolysis product present in the extraction. We quantified the concentration of terephthalate units by adding 1,4-dimethoxybenzene as an internal standard to the extracted solutions. To relate the quantified number of terephthalate protons to the number of terephthalate protons that was added to the hydrolysis experiment in the form of PBAT, we extrapolated the amounts that we quantified in the three consecutive extractions with an exponential decay fit. Extrapolating for 10 extractions resulted in a recovery of 86 ± 8 %. In summary, this finding showed that BT is the predominant terephthalate-containing product of the hydrolysis of PBAT by FsC. Thereby, this experiment matches the extents of cleaved ester bonds we detected by pH-stat titration (**Figure 1**).

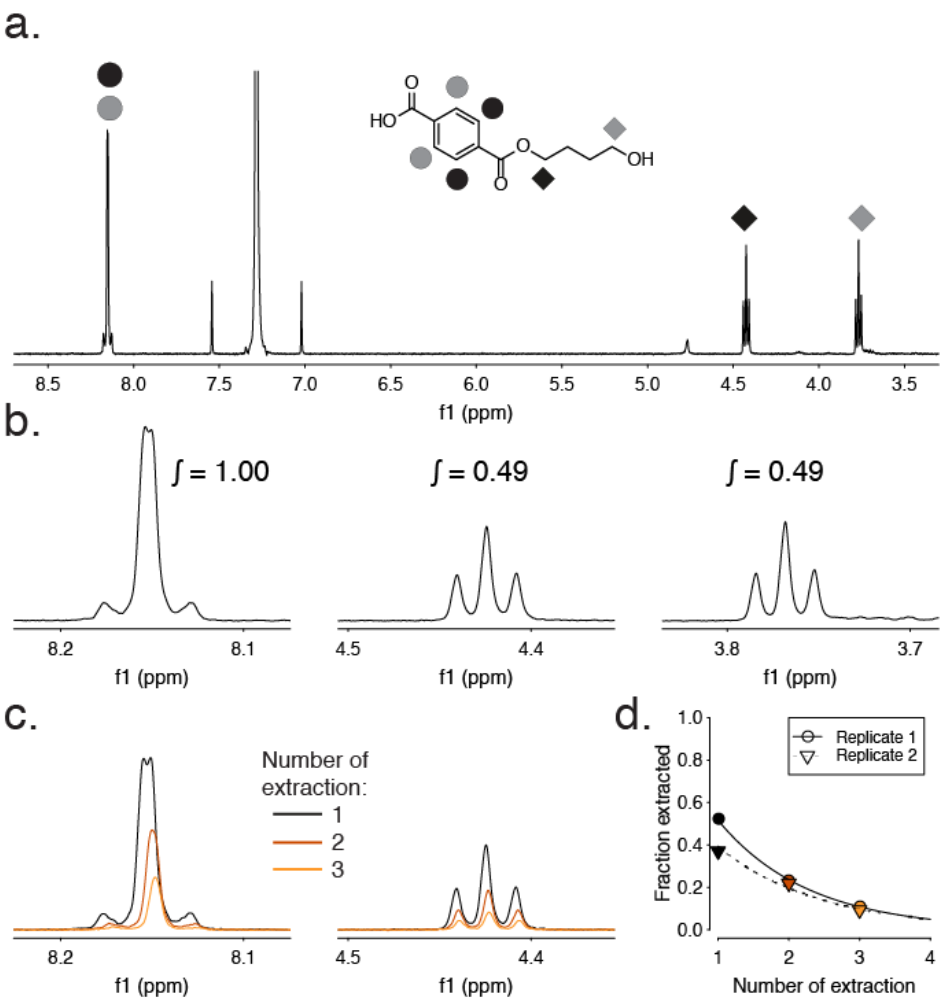

Figure S10. ^{1}H NMR analysis of the products from the enzymatic hydrolysis of untreated poly(butylene adipate-co-terephthalate) (PBAT) after liquid-liquid extraction. **a.** ^{1}H NMR spectrum of hydrolysis products and structural formula of the butanediol-terephthalate dyad (BT). The symbols depict the assignment of the characteristic protons to the peaks in the spectrum. **b.** Enhanced regions containing the spectral peaks assigned to the characteristic protons of BT and their integration values. **c.** Enhanced regions of two spectral peaks assigned to the characteristic protons of BT. Spectra obtained after consecutive extractions are shown in different colors. **d.** Fraction of extracted PBAT-derived terephthalate for three consecutive extractions of duplicate hydrolysis experiments. The lines depict exponential fits for the points.

Quantification of enzymatic PBAT hydrolysis by TOC measurements

To confirm the trend observed with pH-stat titration experiments (i.e., enzymatic hydrolyzability of PBAT decreases with increasing UV irradiation), we performed complementary experiments, in which we assessed enzymatic PBAT hydrolysis by quantifying the hydrolysis products that were released into the solution by total organic carbon (TOC) measurements of aliquots sampled from the hydrolysis solution during the experiment (**Figure S11**). Although this is a convenient approach, we note that it is more error-prone and less time-resolved than the pH-stat titration approach. Nonetheless, these experiments confirmed that films that had been irradiated for 6 h were hydrolyzed at a similar rate to untreated films, whereas longer irradiation times significantly reduced the rates at which PBAT films were hydrolyzed by FsC. We note that the small differences between the results of the pH-stat titration experiments and the results of the TOC-based experiments were likely due to the different measurement principles; while TOC measurements detect all carbon that is released into the solution (i.e., also soluble fragments that were formed by the photochemical scission of PBAT chains), pH-stat titration measures all protons released into the solution (i.e., also if no organic hydrolysis product is small enough to be released into the solution). Due to the improved time resolution and robustness of the pH-stat titration approach, we used the data of the TOC data to confirm the major trends found with pH-stat titration experiments.

We also used the TOC-based approach to assess if the rate of PBAT hydrolysis is increased when the concentration of enzyme is increased (**Figure S12**). The results of this experiment demonstrated that that the hydrolysis rate did not increase with increasing enzyme concentration, which confirmed that all experiments in the manuscript were performed under surface-saturation by the enzyme. For all experiments monitored by solution TOC analysis, we performed background measurements of the incubation medium and enzyme in order to effectively subtract out their contribution to the measured carbon content.

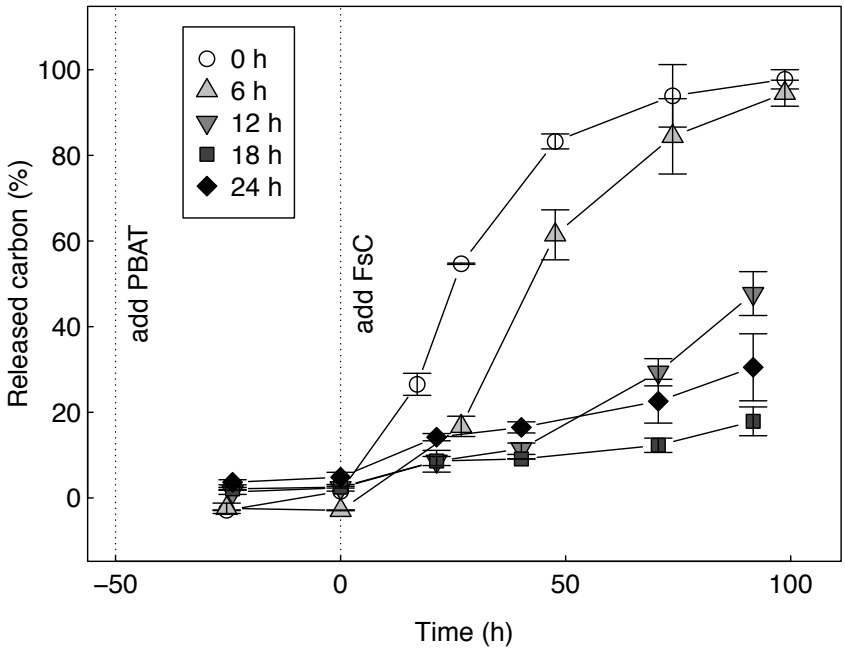

Figure S11. Hydrolysis of irradiated poly(butylene adipate-co-terephthalate) (PBAT) films by *Fusarium solani* cutinase (FsC). The plot shows the cumulative amount of organic carbon that was released into the solution, relative to the amount of organic carbon in the PBAT film initially added to the experiment. We quantified released carbon by total organic carbon (TOC) measurements of the hydrolysis solution. PBAT films were irradiated on both sides with UV light for the time indicated in the legend. PBAT films and FsC were added to the system at the times indicated by the vertical dashed lines at –50 and 0 h, respectively. Error bars represent the ranges of independent duplicates from their means.

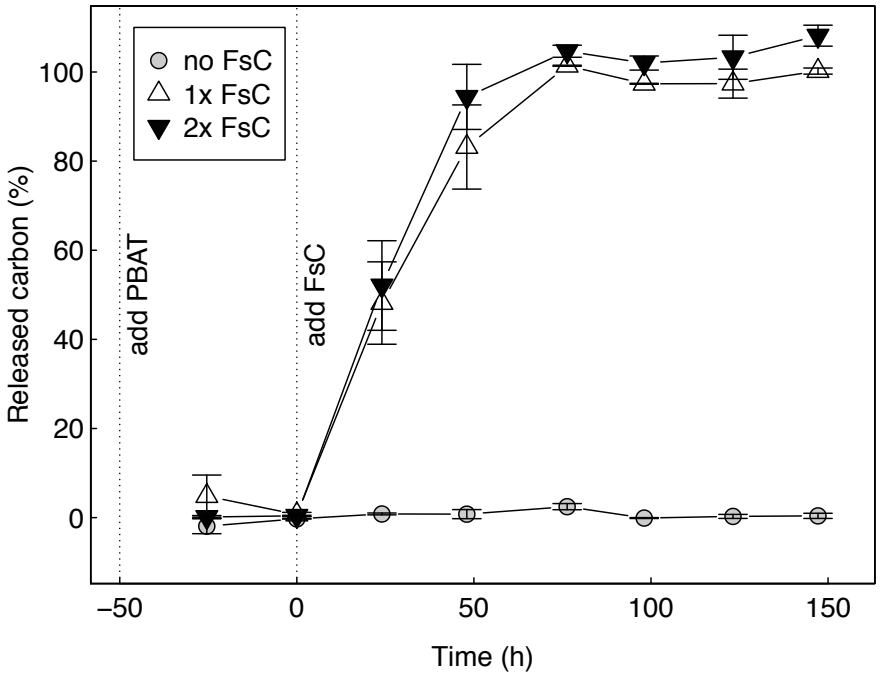

Figure S12. Hydrolysis of poly(butylene adipate-co-terephthalate) (PBAT) films by *Fusarium solani* cutinase (FsC). The plot shows the cumulative amount of carbon that was released into the solution, relative to amount of carbon in the PBAT film, quantified by total organic carbon (TOC) measurements of the hydrolysis solution. PBAT films and FsC were added to the system at the times indicated by the vertical dashed lines at -50 and 0 h, respectively. Error bars represent the ranges of independent duplicates from their means. Circles, triangles, and inverted triangles represent experiments with different concentrations of FsC (i.e., zero, standard concentration used in all experiments of the manuscript, and doubled concentration, respectively).

DSC and WAXS analysis of untreated and irradiated PBAT films

We investigated the effect of UV irradiation on the crystallinity of PBAT by employing two complementary methods: differential scanning calorimetry (DSC) and wide-angle x-ray scattering (WAXS). The % crystallinity of a polymer is directly related to the enthalpy of melting ΔH_m. [5] The ΔH_m values obtained by DSC indicated that the % crystallinity does not change significantly after UV-irradiation (**Figure S13** and **Table S1**). We sought to corroborate the DSC results using WAXS. The data obtained by WAXS for the untreated and irradiated PBAT samples is in good agreement with the expected crystal structure for PBAT: the crystalline domains are dominated by poly(butylene terephthalate) (PBT) crystals rather than poly(butylene adipate) crystals. The reported values for the triclinic unit cell (α form) of PBT are a = 4.83 Å, b = 5.94 Å, c = 11.59 Å, α = 99.7°, β = 115.2°, and γ = 110.8°.[6] Using very slightly modified values (a = 4.89 Å, b = 5.94 Å, c = 11.78 Å, α = 100.3°, β = 115.0°, and γ = 111.1°), the experimental data can be indexed according to the expected reflections from this unit cell. There is good agreement between these reflections and the observed peaks (**Figure S14**). Importantly, there was no change in the crystal structure with UV irradiation and very little change in the peak intensities, which suggested that the % crystallinity remains constant with prolonged UV exposure (**Figure S15**). Based on the DSC and WAXS results, we therefore ascribe the decrease in hydrolyzability with increasing irradiation time primarily to the reduced chain flexibility due to photo-crosslinking.

We furthermore note that the DSC measurements revealed that the melting temperature T_m for the crystalline domains, which has previously been shown to negatively correlate with enzymatic hydrolyzability,[7-10] decreased with increasing UV exposure time (**Table S1**). Although the data shown is for the first heat, the same trend was observed after erasing the thermal history (i.e., on the second heat). Due to the low % crystallinity of commercial PBAT films (e.g., EcoFlex, 11%), there are few crystallites present and the network that is formed from UV-irradiation is thus essentially a network of randomly oriented chains. In such networks, it has been empirically observed that a small degree of cross-linking can drastically reduce the melting temperature (both onset and maximum), which has been explained by a change in the entropy of fusion. [5] This melting point depression trend continues—though not as drastically—as cross-link density is increased.

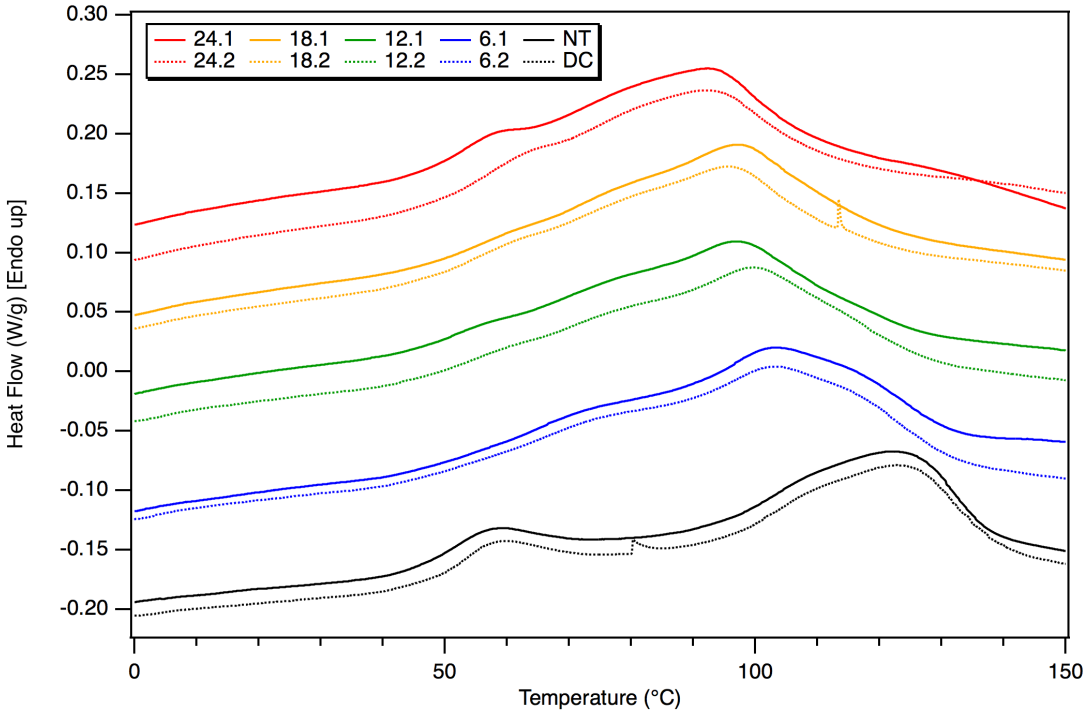

Figure S13. An overlay of differential scanning calorimetry (DSC) traces of untreated PBAT (denoted NT), a dark control (DC), and PBAT irradiated on both sides with UV light for the time indicated in the legend (i.e., 6-24 h). Duplicate measurements for the irradiated films are shown as solid and dotted lines in the same color (denoted X.1 or X.2, where X is the irradiation time in hours). Traces are vertically scaled for clarity.

Table S1. Thermal properties of PBAT samples measured by DSC.

Sample ID[a]	**ΔH_m (J/g)**[b]	**T_m (°C)**[c]
NT	29	121
DC	27	123
6.1	28	103
6.2	31	103
12.1	28	97
12.2	29	99
18.1	27	97
18.2	26	99
24.1	27	92
24.2	25	91

[a] Nomenclature: untreated PBAT is denoted NT, a dark control is denoted DC, and duplicate samples of UV-irradiated are denoted X.1 or X.2, where X is the irradiation time in hours. [b] Enthalpy of melting was determined by integrating the signal produced by the melting transition. [c] The melting temperature was defined as the global maximum of the melting transition.

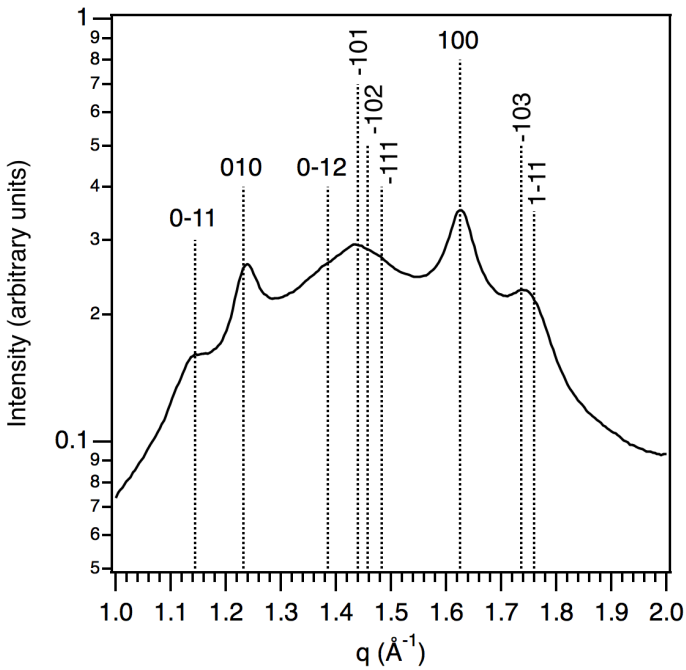

Figure S14. Wide-angle x-ray scattering (WAXS) data of untreated poly(butylene adipate-co-terephthalate) (PBAT) with Miller indices shown for the expected reflections of the triclinic poly(butylene terephthalate) (PBT) unit cell (α form). The parameters used to index the peaks were: a = 4.89 Å, b = 5.94 Å, c = 11.78 Å, α = 100.3°, β = 115.0°, and γ = 111.1°. Although poorly developed along the c axis, the peaks corresponding to the a and b axis are very distinct (100 and 010, respectively). The underlying broad bump is due to scattering from amorphous material.

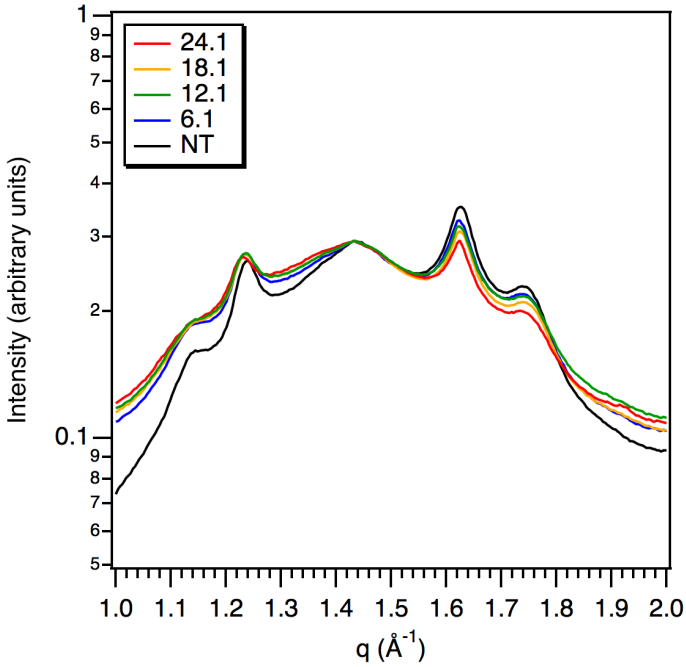

Figure S15. Wide-angle x-ray scattering (WAXS) data of untreated poly(butylene adipate-co-terephthalate) (PBAT) (denoted NT) and PBAT irradiated on each side for the time indicated in the legend (6-24 h). The irradiated PBAT curves were vertically shifted to align with the NT data at q = 1.432 Å^{-1}.

Chloroform-soluble and chloroform-insoluble mass fractions of irradiated PBAT films.

The degree of cross-linking is commonly evaluated by swelling experiments. Therefore, we sought to complement our rheological data by evaluating the chloroform-soluble and chloroform-insoluble mass fractions (i.e., sol and gel fractions) for the PBAT samples. As expected, the untreated PBAT is fully soluble (i.e., sol fraction = 1) and the irradiated PBAT samples are only partially soluble due to photochemical cross-linking. Longer irradiation times produce samples with higher gel fractions. In each case, the mass balance for these experiments was confirmed by summing the gel and sol fractions (**Figure S16**).

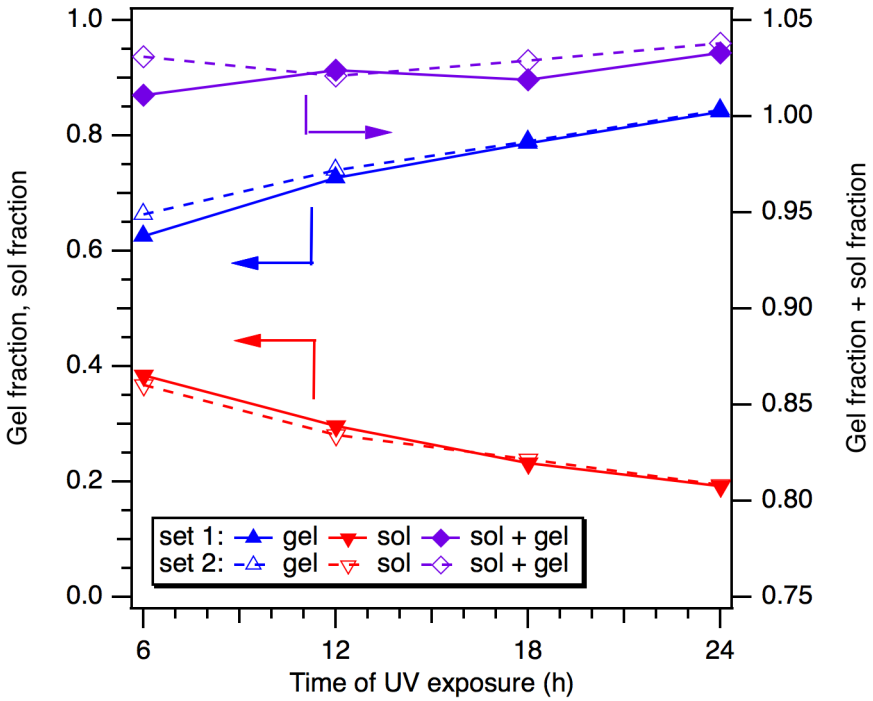

Figure S16. Chloroform-insoluble (i.e., gel), chloroform-soluble (i.e., sol) and total (i.e., sol+gel) mass fractions of PBAT films that were irradiated on both sides for the time indicated on the x-axis. Duplicate experiments are depicted as open and closed symbols in the same color.

SEC analysis of untreated PBAT and the soluble fraction of irradiated PBAT films

We expected that the UV irradiation of untreated PBAT would cause simultaneous cross-linking and fragmentation events, which would generate an insoluble PBAT network containing chain fragments. To confirm the presence of these fragments, we analyzed the soluble fractions of the irradiated PBAT samples and compared them to untreated PBAT. Indeed, SEC analysis revealed a shift toward longer elution volumes for the soluble fractions that were from longer irradiation times. This finding strongly supports the conclusion that prolonged irradiation resulted in lower molar mass PBAT fragments (**Figure S17**).

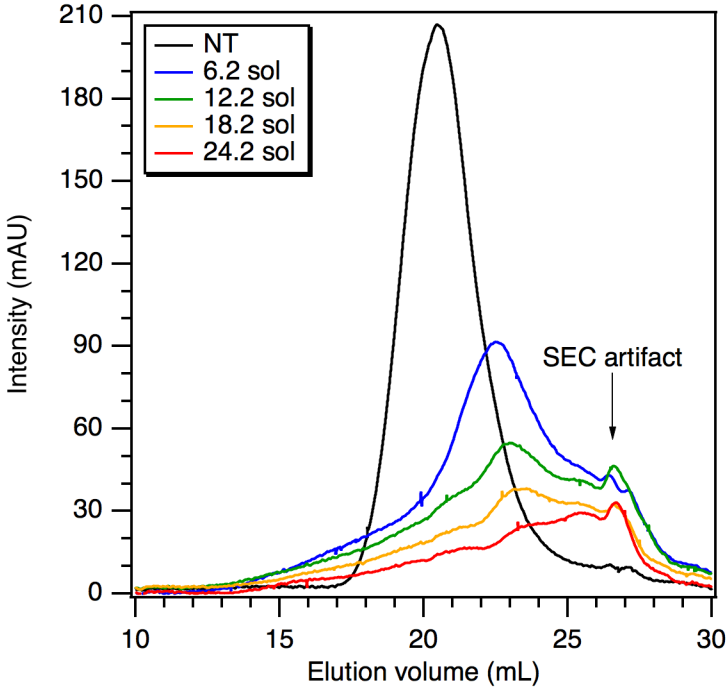

Figure S17. An overlay of size-exclusion chromatography (SEC) traces of untreated PBAT (denoted NT) and sol fractions from the PBAT samples irradiated with UV light for 6, 12, 18, and 24 h per side. There is an artifact at *ca.* 26.5 mL that contributes to the signal; it is seen in all traces obtained on this size-exclusion chromatograph.

Experimental details and raw data for dynamic mechanical thermal analysis (DMTA) measurements

A typical procedure for each DMTA measurement was as follows. The transducer was zeroed and tared at room temperature with the oven closed after the stream of nitrogen gas (from the liquid nitrogen chamber) equilibrated. A PBAT sample was then loaded in the tensile fixtures using a torque wrench (40 cN·m) to ensure that the sample maintained continuous contact with the fixtures during the temperature sweep. Liquid nitrogen was used to cool the sample to -80 °C, and the axial force was continuously adjusted to 20.0 g (sensitivity 1.0 g) to ensure no buckling of the film. The proportional force mode was set to force tracking to maintain an axial force that was at least 100% greater than the dynamic oscillatory force. The compensate for modulus feature was not used and the adjustment time out for the axial force was set to 4.0 s. The minimum axial force was set to 2.0 g and the minimum and maximum oscillatory force were set to 1.0 g and 20.0 g, respectively. The strain adjust was set to 30% with minimum and maximum strain values of 0.05% and 5.0%, respectively. The sample was then heated to 200 °C at a rate of 5 °C·min^{-1} at an angular frequency of 6.28 rad·s^{-1} (1 Hz). Data acquisition was performed in correlation mode with 0.5 delay cycles and 0.5 s of delay time.

The data below show the storage modulus E' (tensile geometry) as a function of temperature for untreated and irradiated PBAT films. Duplicate samples were prepared for all irradiated films; the nomenclature is *X.Y*, where *X* denotes the irradiation time (per side) in hours and *Y* denotes the two sets of samples. Unlike the untreated sample, the irradiated PBAT samples maintain a relatively steady plateau modulus after they undergo their melting transitions (**Figure S18**). This steady modulus is due to the photo-crosslinking caused by UV irradiation. Longer irradiation times generate samples with higher cross-link densities and thus higher storage moduli (**Figure S19**). At a given temperature (here 150 °C), the storage modulus can be used to calculate the average molar mass between cross-links M_x (inversely proportional to the cross-link density), which ranges from approximately 14 to 3 kg/mol (**Figure S20**).

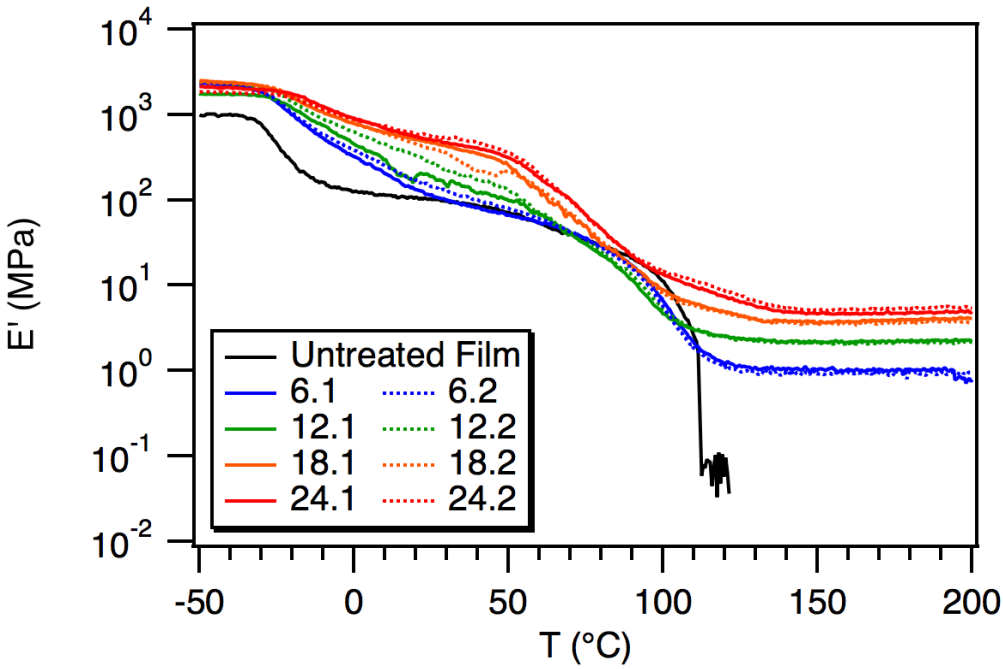

Figure S18. Dynamic thermal mechanical analysis (DMTA) of irradiated and untreated poly(butylene adipate-co-terephthalate) (PBAT) films. DMTA was performed on parts of the film samples used for enzymatic hydrolysis experiments (Figure 1); films were irradiated with UV light for the time indicated in the legend (i.e., 6-24 h per side). Duplicate measurements for the irradiated films are shown as solid and dotted lines in the same color.

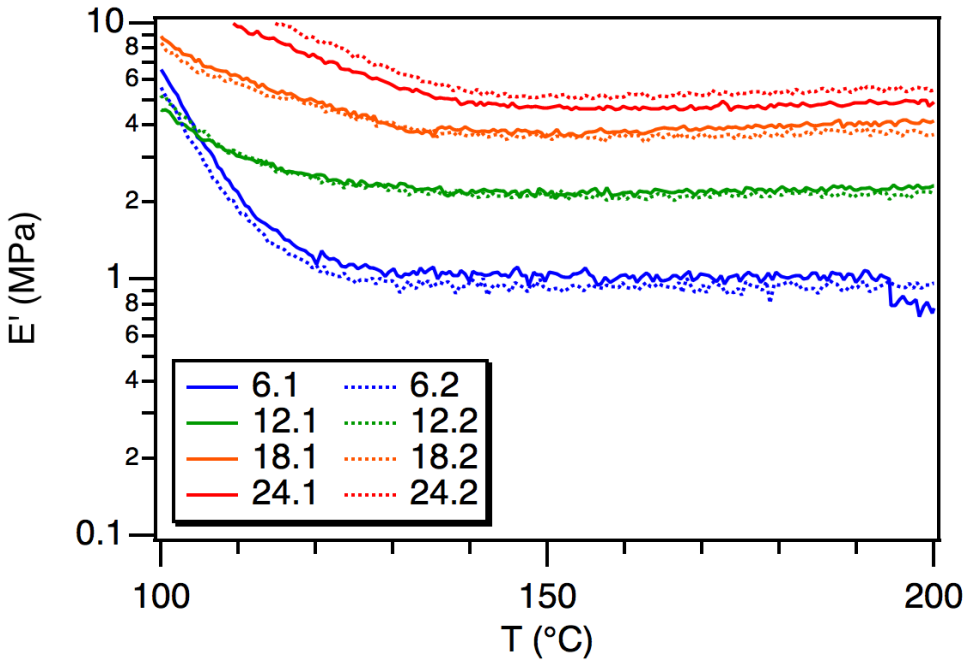

Figure S19. Enhanced view of the dynamic thermal mechanical analysis (DMTA) of irradiated poly(butylene adipate-co-terephthalate) (PBAT) films above their melting transition. The figure represents an expansion of the data shown in Figure S18. Both sides of the films were irradiated for the time indicated in the legend (i.e., 6-24 h). Duplicate measurements for the irradiated films are shown as solid and dotted lines in the same color.

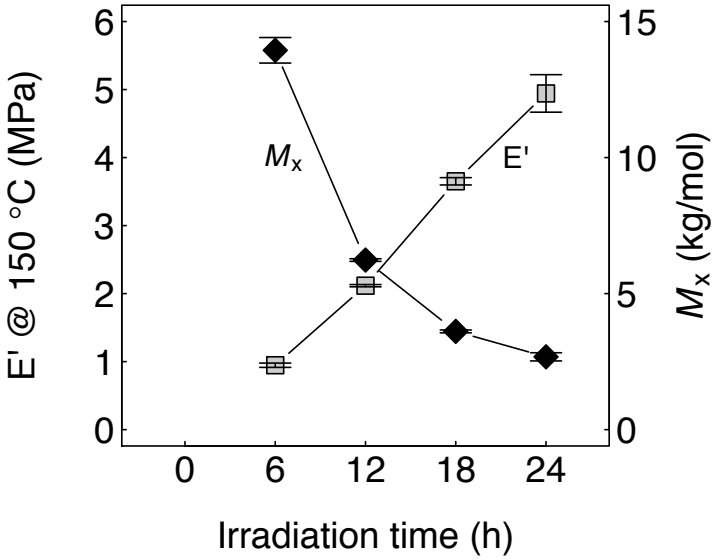

Figure S20. Graphical depiction of the storage modulus (*E′*) at 150 °C measured by dynamic mechanical thermal analysis (DMTA) and the corresponding average molar mass between cross-links (M_x) for irradiated poly(butylene adipate-co-terephthalate) (PBAT) films. between two crosslinks. Error bars represent the ranges of independent duplicate measurements from their means.

Comparison of sunlight irradiation to irradiation in the Rayonet photoreactor

To frame our experimental results in a more environmentally-relevant context, we compared the initial rate of the formation of chloroform-insoluble poly(butylene adipate-co-terephthalate) (PBAT) (i.e., gel fraction) between films that were irradiated by sunlight and films that were irradiated in the photoreactor (**Figure S21**). We note that these films were only irradiated on one side and that these measurements were performed differently than the gel fraction measurements described in the manuscript (see Section S1 for experimental details). As the purpose of these experiments was to ensure that cross-linking is triggered by natural sunlight and to provide a comparison between natural and artificial light exposures, we considered gel fraction measurements, which can be done much more rapidly than dynamic mechanical thermal analyses, to be sufficient.

During the initial 4 h of irradiation in the photoreactor, the gel fraction of PBAT films increased linearly with a slope of 11.4%/h. We compared this rate to the rate of gel formation during the first two weeks of the sunlight irradiation experiment (linear phase). The number of sunny days during these two weeks was derived from irradiance data that was collected on the roof of our institute's building (i.e., the same location as the sunlight-irradiation experiments were performed, see text to **Figures S22** and **S23** for details). These estimations suggested that a 12 h irradiation in the photoreactor corresponds to ~26 sunny days in central Europe in early June.

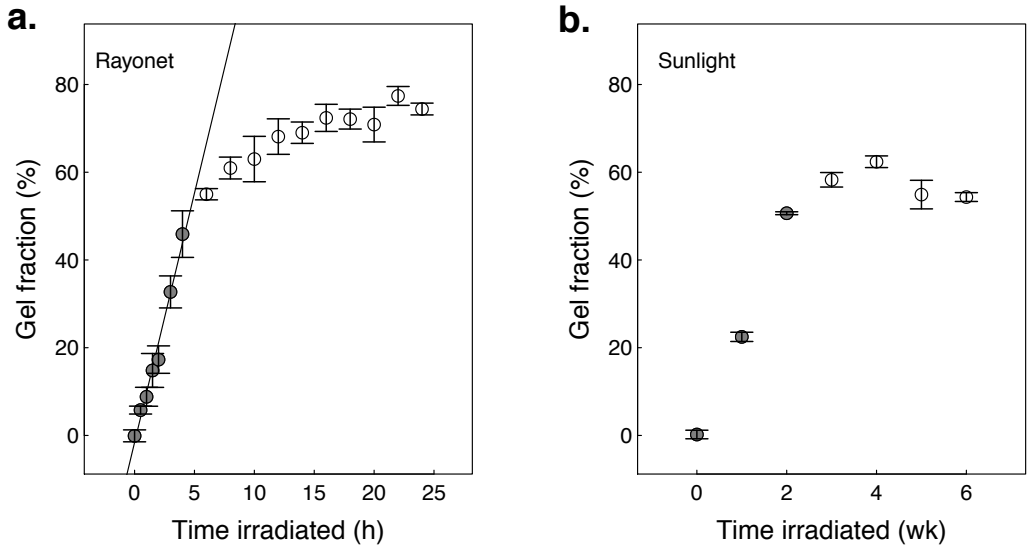

Figure S21. Chloroform-insoluble mass (i.e., gel) fractions of PBAT films that were irradiated on one side for the time indicated on the x-axes either in the Rayonet photoreactor (panel a) or by sunlight (panel b). Error bars represent standard deviations

of triplicates. Filled circles represent the data points comprising the linear phase of gel formation; these data were thus used for the quantitative comparison.

Irradiance data for sunlight irradiation experiment

To determine the number of sunny days during the sunlight-irradiation experiment, we used illuminance data that researchers from the Institute of Atmospheric and Climate Science (IAC) at ETH Zurich collected on the roof of our institute's building (**Figure S22**). The number of sunny days per week was calculated by dividing the integral of the illuminance curves for the entire week by the integral of the illuminance curve measurement on June 7 (i.e., an almost perfectly sunny day, **Figure S23**).

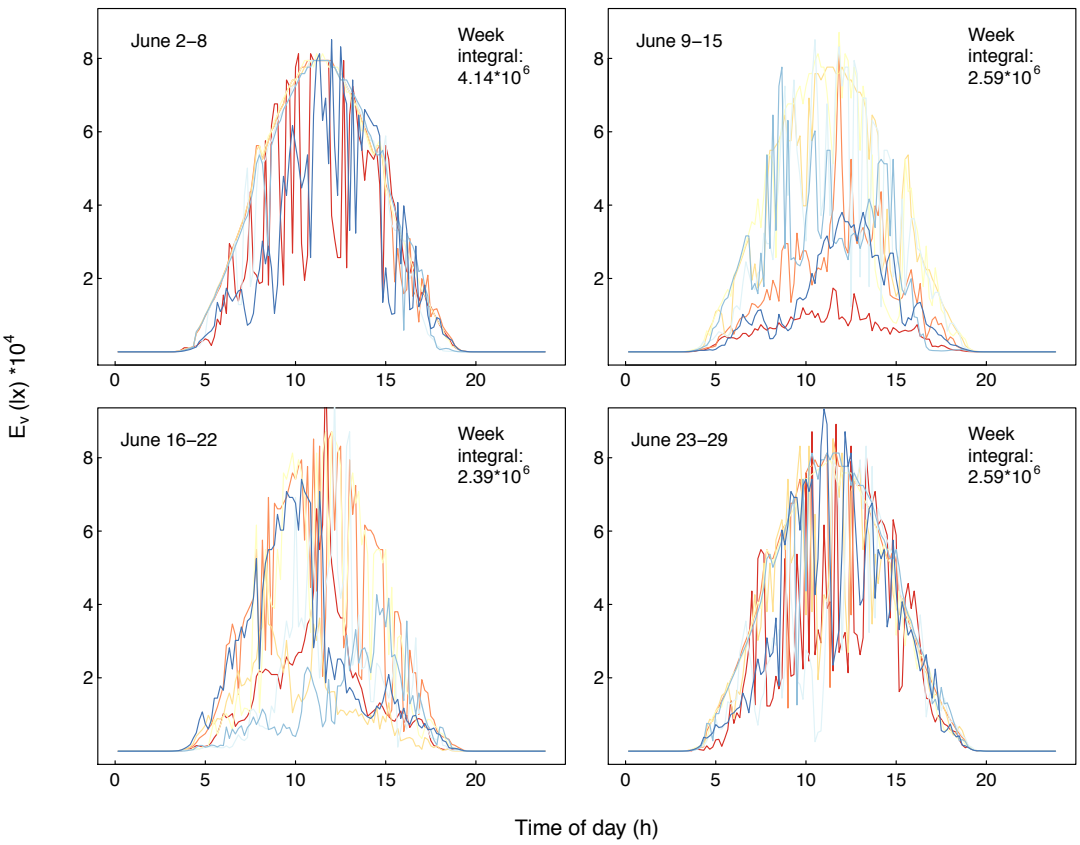

Figure S22. Illuminance data collected on the roof of our institute's building in Zurich Switzerland on June 2015. The curve for each day of a week is shown in a different color. The integrals of the curves (over the entire week) are provided in the top right corner of each panel. The dates are provided on the top left corner of each panel. Data was collected by researchers from the Institute of Atmospheric and Climate Science (IAC) at ETH Zurich.

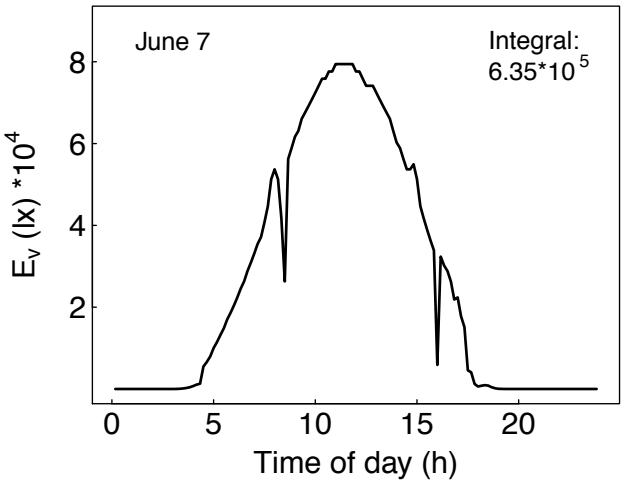

Figure S23. Illuminance data collected on the roof of our institute's building in Zurich Switzerland on June 7, 2015. The integral of the curve is provided in the top right corner. Data was collected by researchers from the Institute of Atmospheric and Climate Science (IAC) at ETH Zurich.

Enzymatic hydrolysis of solvent-cast and photostabilized PBAT films

To study whether the presence of a photostabilizing additive reduces the effect of UV irradiation on the enzymatic hydrolysis of poly(butylene adipate-co-terephthalate) (PBAT), we solvent casted PBAT films with and without 2% (w/w) of 2-(2-benzotriazolyl)-4-methylphenol and assessed the hydrolysis of these films by *Fusarium solani* cutinase (FsC) using pH-stat titration (**Figure S24**). These experiments revealed that FsC-mediated hydrolysis after UV irradiation was indeed faster for photostabilized films than for films that did not contain the photostabilizer. Photochemical production of carboxylic acids was reduced - but not completely inhibited - by the addition of the photostabilizer to the films. Enzymatic hydrolysis rates of untreated films were not significantly different between photostabilized and non-photostabilized films.

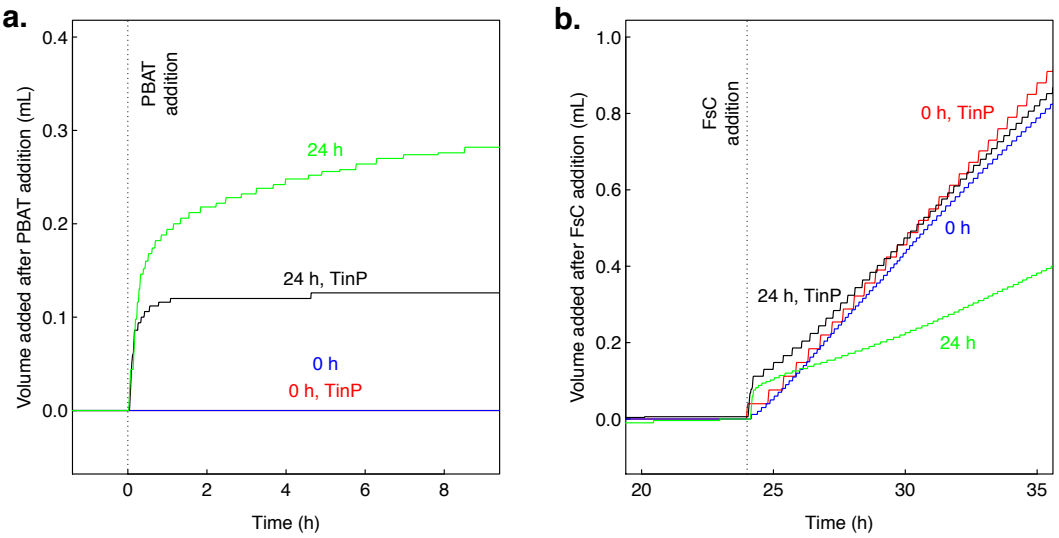

Figure S24. Hydrolysis of solvent-cast poly(butylene adipate-co-terephthalate) (PBAT) films—both irradiated and non-irradiated—by *Fusarium solani* cutinase (FsC). Both panels show the cumulative volume of potassium hydroxide solution that was added to keep pH 7 constant. **a.** Volume added after the addition of the solvent-casted PBAT films to the solution (addition is represented by the vertical dashed line at t=0 h). **b.** Volume added after the addition of FsC to the solution (addition is represented by the vertical dashed line at t=24 h). For the experiments represented by black and green curves, each side of the PBAT films was irradiated with UV light for 24 h. Red and blue curves represent dark controls. Films used for experiments represented by red and black curves contained 2% (w/w) of the photostabilizer 2-(2-benzotriazolyl)-4-methylphenol. Duplicate experiments exhibited similar rates, but were not included for the sake of clarity.

References

(1) Laszakovits, J. R.; Berg, S. M.; Anderson, B. G.; O'Brien, J. E.; Wammer, K. H.; Sharpless, C. M. p-Nitroanisole/Pyridine and p-Nitroacetophenone/Pyridine Actinometers Revisited: Quantum Yield in Comparison to Ferrioxalate. *Environ. Sci. Technol. Lett.* **2017**, *4* (1), 11–14.

(2) Herrera, R.; Franco, L.; Rodríguez-Galán, A.; Puiggalí, J. Characterization and degradation behavior of poly(butylene adipate- co-terephthalate)s. *J. Polym. Sci. A Polym. Chem.* **2002**, *40* (23), 4141–4157.

(3) Sangroniz, A.; Sangroniz, L.; Aranburu, N.; Fernández, M.; Santamaria, A.; Iriarte, M.; Etxeberria, A. Blends of biodegradable poly(butylene adipate-co-terephthalate) with poly(hydroxi amino ether) for packaging applications_ Miscibility, rheology and transport properties. *European Polymer Journal* **2018**, *105*, 348–358.

(4) Kuwabara, K.; Gan, Z.; Nakamura, T.; Abe, H.; Doi, Y. Crystalline/Amorphous Phase Structure and Molecular Mobility of Biodegradable Poly(butylene adipate-c o-butylene terephthalate) and Related Polyesters. *Biomacromolecules* **2002**, *3* (2), 390–396.

(5) Mandelkern, L. *Crystallization of Polymers*, Second Edition. Cambridge University Press: New York, 2004; Vol. 1.

(6) Yokouchi, M.; Sakakibara, Y.; Chatani, Y.; Tadokoro, H.; Tanaka, T.; Yoda, K. Structures of Two Crystalline Forms of Poly(butylene terephthalate) and Reversible Transition between Them by Mechanical Deformation. *Macromolecules* **1976**, *9* (2), 266–273.

(7) Marten, E.; Müller, R.-J.; Deckwer, W.-D. Studies on the enzymatic hydrolysis of polyesters. II. Aliphatic–aromatic copolyesters. *Polymer Degradation and Stability* **2005**, *88* (3), 371–381.

(8) Zumstein, M. T.; Rechsteiner, D.; Roduner, N.; Perz, V.; Ribitsch, D.; Guebitz, G. M.; Kohler, H.-P. E.; McNeill, K.; Sander, M. Enzymatic Hydrolysis of Polyester Thin Films at the Nanoscale: Effects of Polyester Structure and Enzyme Active-Site Accessibility. *Environ Sci Technol* **2017**, *51* (13), 7476–7485.

(9) Zumstein, M. T.; Kohler, H.-P. E.; McNeill, K.; Sander, M. High-Throughput Analysis of Enzymatic Hydrolysis of Biodegradable Polyesters by Monitoring Cohydrolysis of a Polyester-Embedded Fluorogenic Probe. *Environ Sci Technol* **2017**, *51* (8), 4358–4367.

(10) Tokiwa, Y.; Calabia, B. P.; Ugwu, C. U.; Aiba, S. Biodegradability of plastics. *Int J Mol Sci* **2009**, *10* (9), 3722–3742.